JOURNAL OF CATALYSIS **177,** 247–258 (1998)
ARTICLE NO. CA982125

Wet Oxidation of Phenolic Solutions over Heterogeneous Catalysts: Degradation Profile and Catalyst Behavior

Safia Hamoudi, Faïçal Larachi,[1] and Abdelhamid Sayari

Department of Chemical Engineering and CERPIC, Université Laval, Ste-Foy, Québec, Canada G1K 7P4

Received November 21, 1997; revised April 20, 1998; accepted April 20, 1998

Removal of phenol by wet air oxidation (WAO) from dilute aqueous solutions was conducted in the presence of oxygen over a 1 wt% Pt/Al_2O_3 and Mn/Ce (7/3) composite oxide catalysts. The reaction was carried out in a batch slurry reactor using pure oxygen as an oxidizing agent under mild reaction conditions, i.e., temperature from 80 to 175°C and oxygen pressure from 0.5 to 1.5 MPa. The platinum catalyst was found to be moderately active, while the Mn/Ce catalyst was remarkably effective in reducing both phenol concentration and total organic carbon. On both catalysts the kinetics of phenol removal was characterized by a fast reaction step followed by a slower one. During WAO reaction, a carbonaceous material was formed and deposited on the catalysts surface. This deposit was characterized by temperature-programmed oxidation coupled to mass spectrometry detection and X-ray photoelectron spectroscopy.

INTRODUCTION

The disposal of wastewater streams containing highly toxic organic pollutants generated by many industrial processes has emerged as a topic of mounting concern in recent years. Among the numerous classes of pollutants, phenols are of particular importance due to their widespread discharge in the environment and to their toxicity to many living organisms (1). The effective removal of such pollutants, for safe discharge, is a challenging task as environmental laws and regulations are becoming more and more stringent. To meet the requirements of these regulations, biotreatment, incineration and adsorption processes are traditionally used. However, toxic pollutants are lethal to the microorganisms employed in bioprocesses (2), whereas incineration (3) or adsorption (4–6) merely transfers the pollution from the liquid to air or to the solid leaving combustion by-products or a contaminated adsorbent for further disposal. Wet air oxidation (WAO) is an attractive method for the treatment of waste streams which are too dilute to incinerate and yet too toxic to treat biologically (7). The basic idea of this technique is to enhance the contact between molecular oxygen, used as an oxidant, and the organic matter to be destroyed. Unfortunately, the efficient removal of pollutants via WAO requires excessive pressures (0.5–20 MPa) as well as high temperatures (150–325°C) (8–10). The use of catalysts makes the process more attractive by achieving high conversion at considerably lower temperature and pressure (11). Homogeneous catalysts such as copper cations are in general very effective WAO catalysts (11–15), but their recovery from the treated effluent requires additional separation costs (16). This drawback can be overcome by using heterogeneous catalysts which are easily recoverable and reusable. Consequently, heterogeneously catalyzed WAO attracted attention because of its potential as an alternate method of purifying wastewaters. Numerous studies in the past three decades were thus devoted to this technique using various solid catalysts. For instance, Sadana and Katzer (17, 18) studied the WAO of phenolic solutions in the presence of 10% CuO/Al_2O_3. Box and Farha (19) patented catalysts consisting of copper, manganese, and lanthanum oxides supported on zinc aluminate spinel for oxidation of acetic acid solutions. Chowdhury and Ross (11) investigated WAO of brewery wastewaters in the presence of different metal oxides and found platinum oxide to be very effective while achieving 92% pollutant reduction. Imamura *et al.* (20, 21) developed several heterogeneous catalysts for wet oxidation and found that Mn/Ce composite oxide catalyst was remarkably active in the oxidation of several refractory pollutants such as acetic acid, pyridine, ammonia, and polyethylene glycol. Interestingly, they found this catalyst to be more active than homogeneous copper catalyst (21). Levec (22) and Pintar and Levec (23) studied the WAO of phenol over mixed copper and zinc oxides supported on alumina, and found this catalyst to be effective for complete removal of phenol within 100 min at 130°C. More recently, Okitsu *et al.* (24) investigated the activity of different noble metals (Pt, Pd, Ru, Rh, Ag) supported on alumina or titania in the oxidation of *p*-chlorophenol; Pt/Al_2O_3 gave the best results by reaching 90% conversion in 30 min of treatment at 150°C.

[1] To whom correspondence should be addressed. E-mail: flarachi@gch.ulaval.ca.

0021-9517/98 $25.00

Many of the investigations dealing with heterogeneously catalyzed WAO reported in the literature have focused mainly on either the evaluation of catalyst performance in terms of percentage abatement of pollutant or the determination of the reaction kinetic parameters. These studies were short on information regarding the catalyst behavior during the WAO reaction toward activity preservation. Although the activity loss induced by catalyst active phase leaching out in the hot acidic WAO reaction media has been addressed in some studies (23–26), the activity loss due to carbonaceous deposits on catalyst surface has been mostly overlooked.

The scope of the present study therefore is to address the following two issues. The first deals with the effect of two heterogeneous catalysts on the WAO of phenolic aqueous solutions: a supported noble metal catalyst (1 wt% Pt/Al_2O_3) and a Mn/Ce composite oxide (molar ratio 7/3). The second issue is to use temperature-programmed oxidation coupled to mass spectroscopy (TPO-MS) and X-ray photoelectron spectroscopy (XPS) techniques to characterize the carbonaceous material deposited on the surface of both catalysts in the course of WAO reaction.

EXPERIMENTAL

Materials

Phenol (99+% purity) was purchased from BDH Co. and was used as received. Purified acetic anhydride and pyridine used for phenol esterification were Baker analyzed reagents. Naphthalene used as an internal standard in GC analyses was supplied by Fisher Scientific Co.. The supported platinum catalyst (1 wt% Pt/Al_2O_3) was supplied by Aldrich Co. Manganese and cerium composite oxide with a molar ratio of 7/3 was prepared by coprecipitation from an aqueous solution of manganese (II) chloride (Fisher Scientific Co.) and cerium (III) chloride (Sigma Chemical Co.) followed by calcination under flowing air at 350°C for 3 h. This procedure is similar to that described by Imamura *et al.* (20).

Catalyst Characterization

The surface area of both catalysts was determined using N_2 adsorption and the BET model (Table 1). The adsorption isotherms were measured using an automated volumetric adsorption analyzer, Omnisorp 100 from Coulter. The platinum dispersion on 1 wt% Pt/Al_2O_3 was determined by pulse chemisorption of hydrogen (10% H_2 in Ar) at ambient temperature using an Altamira AMI1 instrument. H_2 pulses were applied to a 1 wt% Pt/Al_2O_3 catalytic bed at regular time intervals (2 min) using a pulse generator (sampling loop of 100 μL), and the amount of H_2 not chemisorbed was monitored by thermoconductivity. Our calculations were based on an adsorption stoichiometry of $H/Pt_s = 1$. The platinum dispersion and the Pt specific surface area (m^2 per g Pt) are given in Table 1.

TABLE 1

Wet Air Oxidation of Phenolic Solutions: Range of Operating Conditions

Initial phenol concentration (g/L)	0.13–10
Catalyst concentration (g/L)	1–5
Oxygen partial pressure (MPa)	0.2–2.5
Temperature (°C)	80–175
Stirrer speed (rpm)	300–900
BET surface area (m^2/g): Pt/Al_2O_3	190
Mn/Ce	107
Pt dispersion for Pt/Al_2O_3 (%)	40
Specific surface area of Pt (m^2/g Pt)	89

The organic species adsorbed on the catalyst during the wet air oxidation reaction were analyzed by TPO using the Altamira AMI1 instrument. In a typical TPO experiment, about 60 to 100 mg of used catalyst was loaded in a U-shaped quartz microreactor which was then installed in a furnace coupled to a temperature controller programmer. The catalyst was first exposed to flowing helium (30 mL/min) and the temperature was raised at a rate of 10°C/min to 120°C and was kept at this temperature for 20 min before being cooled to room temperature. This first treatment was conducted at a relatively low temperature in order to remove physisorbed water from the catalyst sample, but without thermally modifying the nature of the deposit. Subsequently, the catalyst was heated under a flowing gas mixture of 5% oxygen in helium at a rate of 8°C/min to 500 or 650°C for the Mn/Ce or the Pt/Al_2O_3 samples, respectively. Analysis of the microreactor outlet gas was performed by thermal conductivity (TCD) and by mass spectrometry using a transpector quadrupole from Leybold Inficon, Inc. The Altamira instrument and the mass spectrometer were both interfaced to personal computers for data acquisition.

XPS spectra for fresh and used catalysts were recorded using a V. G. Scientific Escalab Mark II system. A Mg$K\alpha$ ($h\nu = 1253.6$ eV) was used as the X-ray source for the Pt/Al_2O_3 and Mn/Ce samples. Survey and detailed spectra were acquired by using channel widths of 1.0 and 0.1 eV, respectively. In order to overcome the sample charging problems, the binding energies (B.E.) of core levels in the observed XPS spectra were referenced to Al2p core level in γ-Al_2O_3 (B.E. = 74.7 eV) and Mn2$p_{3/2}$ core level in MnO_2 (B.E. = 642.2 eV).

Apparatus and Procedure

A schematic diagram of the apparatus used in this study is shown in Fig. 1. The main part of the system was a 300-mL stainless steel high pressure Parr autoclave (model 4842, Parr Instrument, Inc.) equipped with an electrical heating jacket, a temperature controller, a pressure transducer, and

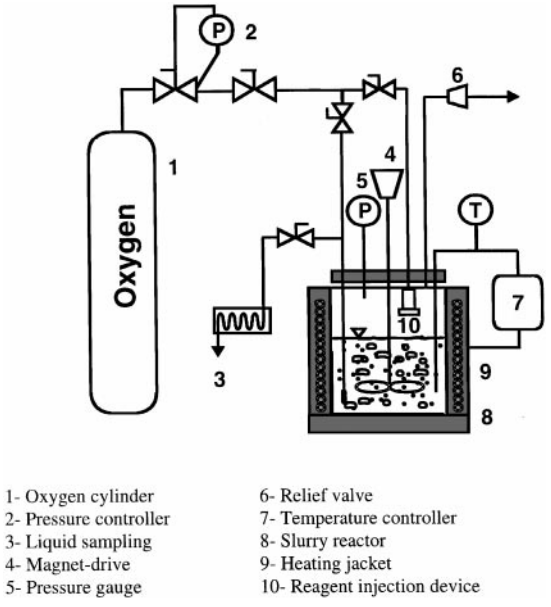

FIG. 1. Experimental setup.

a magnetically driven four-blade turbine type impeller. The autoclave was operated batchwise. The system was also equipped with a reagent injection device connected to a secondary oxygen inlet allowing addition of phenol after the system had equilibrated to reaction conditions.

In a typical run, the autoclave was loaded with 100 mL distilled water and a known amount of catalyst. A predetermined volume of a 25 g/L phenol solution was introduced into the reagent injection vessel. The autoclave was then sealed, pressurized with oxygen, and heated to the desired temperature. Continuous agitation of the slurry at 900 rpm during the heating period allowed its complete saturation with oxygen before the beginning of the reaction. The concentrated phenol solution was then introduced into the reactor at once by applying an overpressure to open the injection device. This moment was taken as the starting time of the reaction. The range of experimental conditions used in this work is shown in Table 1. To eliminate the effect of sampling on the reaction conditions, a single representative sample was withdrawn at a preset reaction time and quenched, and the experiment was stopped. To avoid the complicating effect of multiple gas and liquid sampling on kinetic measurements, a separate experiment was used for each measurement.

Liquid samples were filtered and analyzed for total organic carbon (TOC) using a Shimadzu 5050 TOC analyzer. The residual phenol concentration was determined after esterification using a Hewlett–Packard GC (HP5890 series II plus) equipped with a mass selective detector (MSD model HP5972). An HP-5MS capillary column (30 m, 0.25 mm, 0.52 μm) was used with as carrier gas ultrahigh purity helium flowing at a rate of 1 mL/min. The temperatures of the injector and the interface between GC and MSD were 250 and 280°C, respectively. The oven temperature was held at 50°C for the first 2 min, then raised to 120°C at a rate of 5°C/min. The sample volume injected was 1 μL and naphthalene dissolved in ethylacetate was used as an internal standard. The experimental relative errors were estimated to be 5% for TOC and 5.6% for phenol.

Both phenol concentration and TOC were expressed with respect to the actual reaction conditions (T, P), taking into account the variation of solution volume caused by solvent evaporation and expansion.

The stability of the Mn/Ce catalyst to leaching of active metal ingredients was verified by analyzing filtered solution samples after complete TOC conversion at each WAO temperature, i.e., 30 min at 130°C, and 120 min at 80–110°C. The concentrations of dissolved Mn and Ce were measured by plasma emission spectrometry using an Optima 3000 spectrometer from Perkin–Elmer.

RESULTS AND DISCUSSION

Tests for External and Internal Transport Limitations

To demonstrate the absence of external mass transfer limitations in supplying phenol and oxygen to the liquid–catalyst interface, WAO experiments were run at six different mixing speeds from 300 to 900 rpm. As shown in Fig. 2, increasing the stirrer speed above 600 rpm did not change the TOC conversion during the WAO of phenol over Mn/Ce at 130°C. All further experiments were therefore performed at the highest agitation speed (900 rpm).

Limitations due to intraparticle diffusion were investigated using standard procedures (27, 29). The initial rates for phenol oxidation were measured at different temperatures over three Mn/Ce catalyst batches with the following particle sizes: 0.023, 0.063, and 0.120 mm. Figure 2 shows that initial rate data for all particle sizes fit the same straight line in the Arrhenius semi-log scale plot. This confirms that,

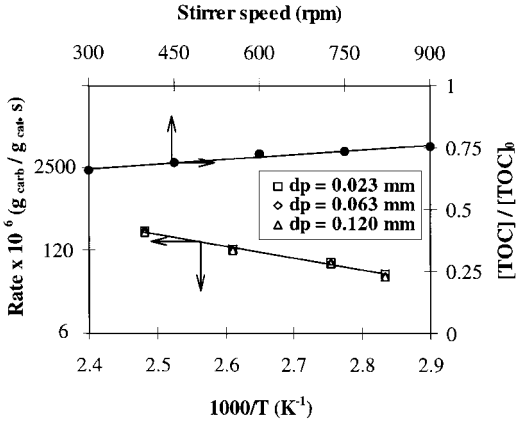

FIG. 2. Evidence of the nonexistence of external and internal mass transfer limitations during phenol WAO over Mn/Ce catalyst (0.5 MPa P_{O_2}).

as any chemically controlled process, the rate constant was independent of the grain size, and therefore intraparticle mass transfer was not the limiting factor in the overall reaction rate (30). The slope of the line corresponded to a mean value of the activation energy of ca. 40 kJ/mol. Hence, all further experiments were conducted using the 0.063 mm grain size.

Effect of Operation Conditions

The effect of temperature was investigated in the range 130–175°C for Pt/Al_2O_3 and 80–130°C for Mn/Ce catalyst. Phenol initial concentrations and oxygen partial pressures were varied in the ranges 0.13–10 g/L and 0.2 to 2.5 MPa, respectively, which led to oxygen-to-phenol stoichiometric ratios in the range 2.5 to 108 far in excess of the requirement for oxidizing phenol into carbon dioxide and water.

Phenol and TOC Removal Profiles

To assess the extent of the (simultaneous) uncatalyzed thermal oxidation of phenol, WAO tests were run without catalysts at 130 and 175°C. As can be seen in Fig. 3, although the uncatalyzed thermal reaction did occur at 175°C (dotted lines), the use of Pt/Al_2O_3 catalyst enhanced appreciably the degradation rate of phenol and TOC during the first 30 min on stream. After 60 min of reaction, the catalytic effect decreased but was still perceptible. The TOC conversions by the catalyzed reaction were ca. 10% higher than those for the uncatalyzed reaction. As will be discussed later, this behavior was ascribed to a fouling type of catalyst deactivation due to the deposition of carbonaceous materials on the catalyst surface. At 130°C, on the other hand, the extent of the uncatalyzed WAO reaction was negligible both for phenol and TOC; less than 7% TOC conversion was achieved after 4 h reaction.

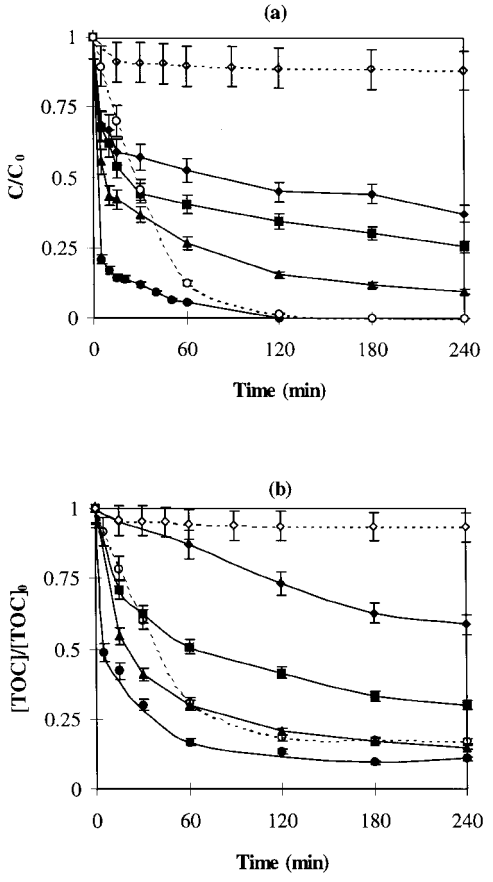

FIG. 3. Effect of temperature on phenol WAO (a) and TOC reduction (b) over Pt/Al_2O_3: (◆) 130°C; (■) 150°C; (▲) 160°C; (●) 175°C; (◇) 130°C uncatalyzed; (○) 175°C uncatalyzed. Solid lines: catalyzed reaction; dotted lines: uncatalyzed; bars show standard deviations on the measurements.

TABLE 2

Initial Activity of Pt/Al_2O_3 and Mn/Ce Catalysts in Terms of Turnover Frequency and Areal Rate

Pt/Al_2O_3		Mn/Ce	
WAO temperature (°C)	Initial TOF (s^{-1})	WAO temperature (°C)	Initial areal rate × 10^8 (mol/m^2 s)
130	0.044	80	0.994
130	0.013[a]		
150	0.096	90	1.912
160	0.148	110	3.828
175	0.287	130	5.659

Note. Reaction conditions were the same as in Figs. 3a and 4a.
[a] $C_0 = 0.2$ g/L.

The performance of the Pt/Al_2O_3 catalyst at different temperatures is shown in Fig. 3 as phenol (Fig. 3a) and TOC (Fig. 3b) relative concentrations in the reaction mixture versus time-on-stream. Under the same conditions, the conversion of phenol is usually higher than that of TOC because of the occurrence of intermediate compounds such as short-chain carboxylic acids which are stable and resistant to further oxidation into CO_2 and H_2O (31, 32). In addition, the effect of temperature on the activity of Pt/Al_2O_3 was expressed in terms of initial turnover frequency (TOF) calculated at 5 min of reaction (Table 2). With increasing temperature, the TOF of reaction increased according to the Arrhenius equation, corresponding to an activation energy of 62 kJ/mol.

In comparison to Pt/Al_2O_3, the Mn/Ce catalyst exhibited higher activity in phenol oxidation. It was active even at temperatures as low as 80°C, which is the lowest temperature reported to date for a heterogeneous catalytic oxidative process for wastewater treatment, excluding photocatalytic and peroxidation methods (33). The effect of temperature on phenol degradation in the presence of Mn/Ce catalyst was thus investigated in the range 80–130°C under a constant oxygen partial pressure of 0.5 MPa as depicted in Fig. 4. It is seen that temperature affects strongly phenol and TOC conversion. Complete removal of the

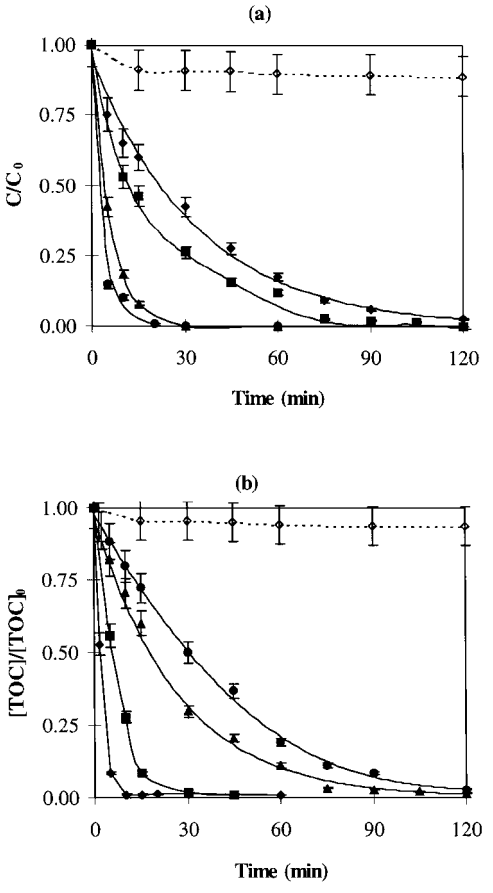

FIG. 4. Effect of temperature on phenol WAO (a) and TOC reduction (b) over Mn/Ce: (◆) 80°C; (■) 90°C; (▲) 110°C; (●) 130°C; (○) 130°C uncatalyzed. Solid lines: catalyzed reaction; dotted lines: uncatalyzed reaction; bars show standard deviations on the measurements.

pollutant occurred within 30 min at 130°C while TOC reduction was 98%. At 80°C, it took slightly less than 2 h to achieve complete conversion of phenol while reaching 97% of TOC reduction. The initial areal rates evaluated for each temperature at 5 min of reaction were between 10^{-8} and 5.6×10^{-8} mol/m^2 s as reported in Table 2. The activation energy deduced from the Arrhenius plot was 40 kJ/mol.

To evaluate the extent of accumulation of intermediate products in the liquid phase during the course of oxidation, phenol concentration was expressed as phenolic carbon (PC) and the difference (TOC-PC), which represents the overall concentration of the intermediates, was normalized to the initial TOC. Figure 5 shows the time course of the accumulation of phenol oxidation intermediates in the presence of the platinum containing catalyst. The (TOC-PC)/TOC_0 curves exhibited a broad peak occurring in the first hour of WAO reaction after which the concentration of the intermediates leveled off. The higher the temperature, the lower the level of the plateau, indicating the formation of less recalcitrant intermediates. In the case of Mn/Ce catalyst, the accumulation of intermediates exhibited a sharp maximum at the very beginning of the oxidation reaction and then decreased very rapidly to low levels. These results were not reported here because the measurements were below the accuracy of the TOC analyzer. The normalized amount of intermediate products was quite different depending on the catalyst and temperature used, and more intermediates persisted in solution for Pt/Al_2O_3 (13–32%) than for Mn/Ce (0–18%). According to Donlagic and Levec (34), the observed shape of the curve of the intermediate products concentration is characteristic of a consecutive reaction. The first step corresponds to the formation of intermediate ring compounds, namely catechol, hydroquinone, and benzoquinones, while the subsequent period represents the formation of ring cleavage intermediates, mainly carboxylic acids (31).

Effect of Oxygen Pressure

The effect of oxygen partial pressure (P_{O_2}) on phenol removal was investigated in the range of 0.2–2.5 MPa at 130°C for both catalysts. To avoid any interference with catalyst deactivation, the influence of oxygen partial pressure was studied in the early stages of reaction, first 15 and 2 min for Pt/Al_2O_3 and Mn/Ce, respectively. A shorter reaction time was chosen for the latter catalyst due to the fact that at 130°C, phenol oxidation was essentially complete within 15 min. Turnover frequencies for the platinum containing catalyst and areal rates for the Mn/Ce catalyst as a function of oxygen partial pressure are shown in Fig. 6. As seen, irrespective of the catalyst used, there was a slight effect of oxygen partial pressure on the catalyst activity up to 1.0 MPa, whereas beyond 1.5 MPa, the rate of phenol oxidation was unaffected by the oxygen pressure level. This is in agreement with Mantzavinos *et al.* (35), who investigated the catalytic oxidation of *p*-coumaric acid over $CuO{-}ZnO/Al_2O_3$ and found

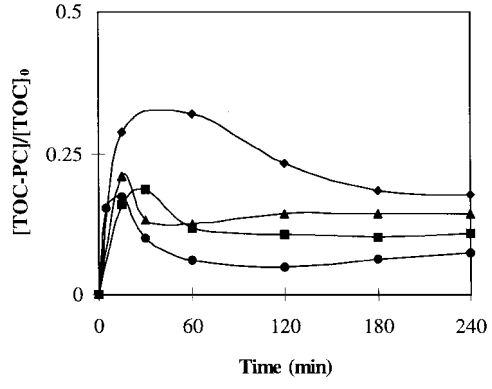

FIG. 5. Relative amount of carbon intermediate species (TOC-PC)/TOC_0 versus reaction time during phenol WAO over Pt/Al_2O_3: (◆) 130°C; (■) 150°C; (▲) 160°C; (●) 175°C.

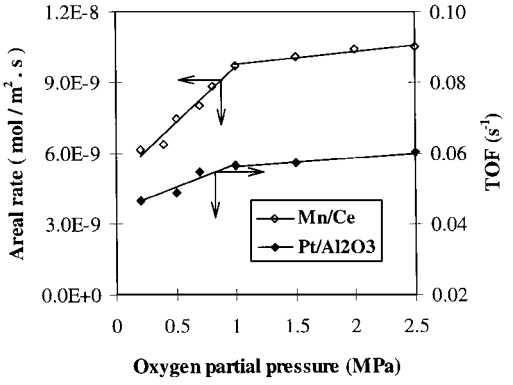

FIG. 6. Effect of oxygen partial pressure on initial TOF and initial areal rates of phenol WAO: (◆) over Pt/Al_2O_3; (◇) over Mn/Ce.

that the effect of oxygen pressure was marginal above 17.3 atm at 130°C.

Effect of Phenol Initial Concentration

The effect of phenol initial concentration was first investigated in the range 0.2–1 g/L at 130°C under 0.5 MPa of oxygen partial pressure in the presence of the noble metal catalyst. The initial turnover frequencies presented in Table 2 indicated a positive dependence of the TOF on phenol initial concentration. The results presented in Fig. 7a as phenol dimensionless concentration versus reaction time indicate that under otherwise identical conditions, the higher the phenol initial concentration, the lower the conversion. As seen in Fig. 7b, a similar but more pronounced behavior was observed with the Mn/Ce catalyst for which the effect of phenol initial concentration was investigated in the range 1–10 g/L at 130°C under 0.5 MPa of oxygen partial pressure. Indeed, in this case, while complete phenol conversion was reached within 30 min on stream with a phenol initial concentration of 1 g/L, only 30–40% conversion was attained with the highest substrate loadings (7.5 and 10 g/L). Furthermore, the degradation profiles observed indicated that the oxidation reaction stopped after ca. 1 h on stream. This may be attributed to a strong catalyst deactivation, the extent of which is highly dependent on the substrate initial concentration. When expressing the reaction rate constant as a function of initial phenol concentration, Pintar and Levec (23, 36) observed the same inhibiting effect of phenol initial concentration on oxidation rate. Nevertheless, when more dilute phenol solutions (0.13–0.40 g/L) were oxidized over 5 g/L of Mn/Ce at a short reaction time (2 min), phenol conversion was independent of phenol initial concentration, indicating that the deactivation free reaction is first order with respect to phenol. This is illustrated in Fig. 8, where the initial areal rates of phenol oxidation exhibit a linear increase with respect to initial phenol concentration, whereas the slopes of the obtained lines are more pronounced for higher temperatures.

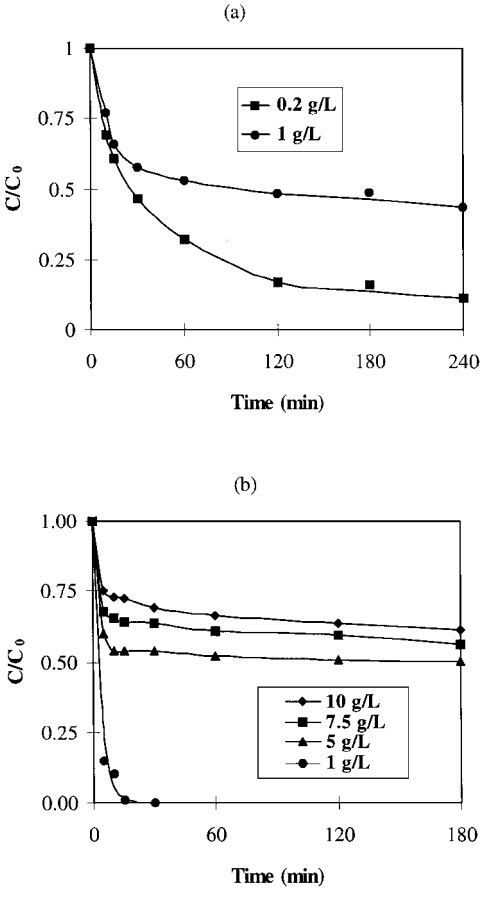

FIG. 7. Dimensionless concentration–time profile of phenol WAO at various phenol initial concentrations over: (a) Pt/Al_2O_3; (b) Mn/Ce. 130°C; 0.5 MPa P_{O_2}; catalyst loading: 5 g/L.

Effect of Catalyst Loading

The effect of catalyst loading was investigated with the Mn/Ce catalyst at 130°C, 0.5 MPa (P_{O_2}) and an initial phenol concentration of 1 g/L. Figure 9 shows the phenol

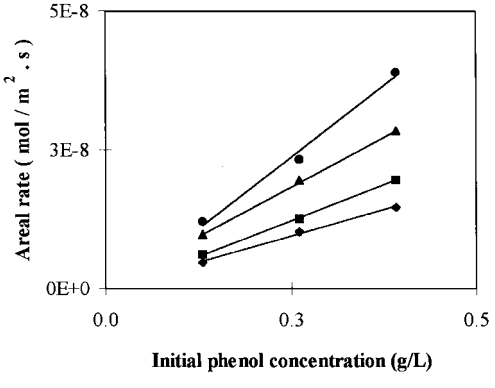

FIG. 8. Linear dependence of initial areal rates of phenol oxidation versus phenol initial concentration at different temperatures over Mn/Ce: (◆) 80°C; (■) 90°C; (▲) 110°C; (●) 130°C. 0.5 MPa P_{O_2}; catalyst loading = 5 g/L.

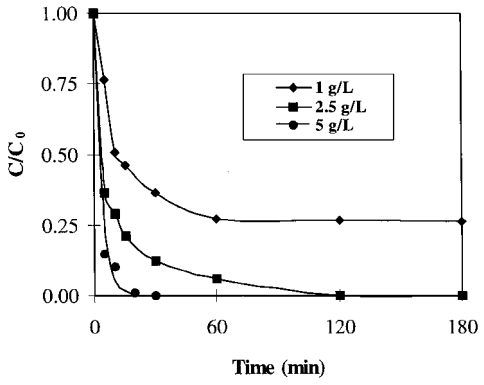

FIG. 9. Dimensionless concentration–time profile of phenol WAO over Mn/Ce at various catalyst loadings: (◆) 1 g/L; (■) 2.5 g/L; (●) 5 g/L. 130°C; 0.5 MPa P_{O_2}; $C_0 = 1$ g/L.

concentration–time profiles at three different catalyst loadings. The initial areal rates were 1.55×10^{-8}, 4.22×10^{-8}, and 5.66×10^{-8} mol/m^2 s for the catalyst loadings of 1, 2.5, and 5 g/L, respectively. It is clearly demonstrated that an increase in catalyst concentration considerably improves the rate of phenol degradation. In fact, while phenol completely vanished within 30 min with 5 g/L Mn/Ce, the maximum conversion achieved with 1 g/L was 70% even after 2 h WAO reaction.

The detrimental effect of phenol initial concentration and the beneficial effect of catalyst loading on phenol conversion suggest that the WAO reaction is highly dependent on the catalyst loading to initial phenol concentration ratio as is typical for heterogeneous catalysts undergoing deactivation. Coke deposition (fouling), surface poisoning, solid state transformations (sintering), and metal leaching are the deactivation scenarios most often encountered (23–26, 37). In WAO reaction, the most probable deactivation mode is coke laydown as will be demonstrated in the next section. Poisoning type of deactivation was unlikely to occur since phenol is an S-, P-, and X-free molecule, the heteroelements known to be poisonous to oxidation catalysts (28). Furthermore, as shown in Table 1, the relatively low WAO temperatures used in the current study exclude the sintering mode of deactivation which is generally observed at higher temperatures (>500°C) (37). Moreover, as shown in Table 3, neither manganese nor cerium leached significantly. Indeed very low concentrations of dissolved metals were detected after completion of the oxidation reaction. The dissolved cerium level was below the detection limits of the instrument. The concentration of dissolved manganese increased with reaction temperature but remained below 0.5% of the total Mn present in the fresh catalyst.

Characterization of the Carbonaceous Deposits

The present study of phenol wet air oxidation over platinum/alumina and Mn/Ce composite oxide catalysts showed that the oxidation rate, though very high at the beginning of the reaction, decreases dramatically after a few minutes on stream. This cannot be accounted for solely by the effect of decreasing phenol concentration nor by the accumulation of more resistant by-products. As highlighted earlier, these two effects are most probably combined with strong catalyst deactivation. This is consistent with recent work by Bond *et al.* (39), who found that reactions of organic compounds on solid catalysts can be accompanied by the formation of heavy by-products which form a carbonaceous deposit on the catalyst surface and cause its deactivation. Pintar and Levec (23), in their study on phenol oxidation over $CuO{-}ZnO/Al_2O_3$ catalyst, observed that after 1 h WAO reaction at 130°C, only 22% of the initial carbon was in the gaseous phase as CO_2, whereas 47% was laid on the catalyst surface in the form of a carbonaceous deposit. The solid deposit was a polymeric product strongly adsorbed on the catalyst and not soluble in conventional organic solvents. In this section, a comparative characterization of the Pt/Al_2O_3 and Mn/Ce catalysts used in this study before and after the WAO reaction was conducted by means of two techniques usually employed in the field of steam reforming catalysts deactivation: TPO-MS and XPS (37).

TPO Analysis

We used this technique in combination with mass spectrometry to determine the burn-off profiles of the carbonaceous materials deposited on the catalysts used in this study. Representative data are shown in Fig. 10. As seen, the consumption of oxygen is mirrored by the formation of CO_2. TPO of the platinum containing catalyst gave one large CO_2 peak starting around 200°C, with maxima at 440 and 540°C for catalyst samples after WAO reactions conducted at 175 and 130°C, respectively. The peak at 540°C suggests that the more difficult-to-remove carbonaceous deposit (or hard coke) is formed on the catalyst surface at the lower WAO temperature. The overall combustion peak can be roughly decomposed into two symmetrical Gaussian peaks, indicating that there were different types of carbon deposits.

TABLE 3

The Extent of Catalyst Leaching at Various WAO Temperatures after Complete TOC Conversion

WAO temperature (°C)	Dissolved Mn[a] (ppm)	Dissolved Ce[b] (ppm)
80	4.9	<0.10
90	5.6	<0.10
110	9.7	<0.10
130	10.0	<0.18

[a] Total Mn in fresh catalyst = 2213 ppm.
[b] Total Ce in fresh catalyst = 1221 ppm.

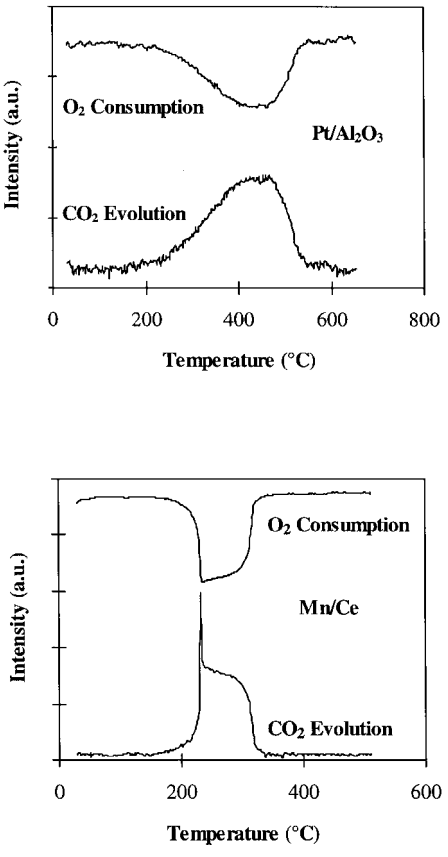

FIG. 10. TPO-MS profiles of used Pt/Al_2O_3 (top) and Mn/Ce (bottom) catalysts.

The first peak with maximum between 280–300°C was assigned to Pt-catalyzed oxidation of carbon which occurs generally at temperatures around 285°C (40–43). This is an indication of participation of the catalyst metal function to the combustion process. The other peak with maximum at temperatures 440–540°C is typical for oxidation of carbon located on alumina support (42). In contrast, as indicated in Fig. 10, the carbonaceous deposit formed over the Mn/Ce catalyst was completely removed below 280°C, indicating that this deposit is much more reactive than that formed on Pt/Al_2O_3 catalyst. The profile of CO_2 formation is characterized by two distinct features: a sharp peak between 200 and 210°C and a broad peak with a maximum between 250 and 280°C. This indicates that either there are at least two kinds of carbon deposits or the deposits located on the Mn and the Ce oxides burn at different temperatures. In fact, according to Menon (43), even with a single reactant and a single catalyst site, different types of coke may be formed and can exhibit different reactivities toward gases such as hydrogen, oxygen, or steam. Pertinent data including the overall oxygen uptake for all samples characterized by TPO, along with their catalytic performance, are given in Table 4. These results show that in the case of fresh Pt/Al_2O_3 sample, no oxygen consumption takes place during TPO within the temperature range of 30–650°C. The oxygen uptake during TPO of a fresh Mn/Ce sample was ca. 8% of the mean value obtained for used samples. Furthermore, this oxygen consumption, which occurs in two stages with maxima at 530 and 610°C, takes place at much higher temperatures than the O_2 consumption during TPO of used catalysts. Moreover, judging from the much lower combustion temperature of deposits accumulated on the Mn/Ce catalyst surface ($T < 300$°C), the regeneration of such a catalyst is likely to be less energy consuming which constitutes a non-negligible advantage in an industrial application.

TABLE 4

TPO Data for Fresh and Used Catalysts

Catalyst	WAO temperature (°C) (reaction time)	TOC conversion (%)	Oxidation temperature[a] (°C)	Oxygen consumption (μmol/g sample)
Pt/Al_2O_3	130 (300 min)	48.0	440; 541	1829
	175 (60 min)	83.2	457	2430
	175 (240 min)	89.1	440	3013
Pt/Al_2O_3[b]	—	—	—	0
Mn/Ce	130 (30 min)	97.7	205; 254	3834
	80 (60 min)	80.9	203; 257	3403
	80 (120 min)	97.2	209; 281	4447
Mn/Ce(b)	—	—	533; 610	307

[a] Temperature of oxidation peak.
[b] Fresh sample.

XPS analysis. High-resolution XPS spectra of the platinum containing catalyst and the Mn/Ce composite oxide before and after reaction at 130°C, 0.5 MPa indicate the emergence of a strong C1*s* peak, confirming the occurrence of an organic overlayer on the surface of used catalysts. For the platinum catalyst, the relative atomic surface composition obtained from XPS data (Table 5) reveals that the carbon content increased from 0.14 to 43% during reaction, thus likely limiting active sites accessibility to WAO

TABLE 5

Fresh and Used Catalysts Surface Composition (%) Determined by XPS Analysis

Catalyst	Component	Before reaction	After reaction
Pt/Al_2O_3	Pt4*d*	0.7 ± 0.002	0.15 ± 0.01
	Al2*p*	39 ± 0.061	22.1 ± 0.05
	O1*s*	60.2 ± 0.062	34.3 ± 0.03
	C1*s*	0.14 ± 0.002	43.5 ± 0.03
Mn/Ce	Mn2*p*	35.2 ± 0.1	1.7 ± 0.07
	Ce3*d*	9.4 ± 0.06	0.50 ± 0.04
	O1*s*	52.9 ± 0.2	50.0 ± 0.7
	C1*s*	2.5 ± 0.01	47.8 ± 0.8

Note. WAO temperature: 130°C; P_{O_2}: 0.5 MPa; reaction time: 2 h for Pt/Al_2O_3 and 30 min for Mn/Ce.

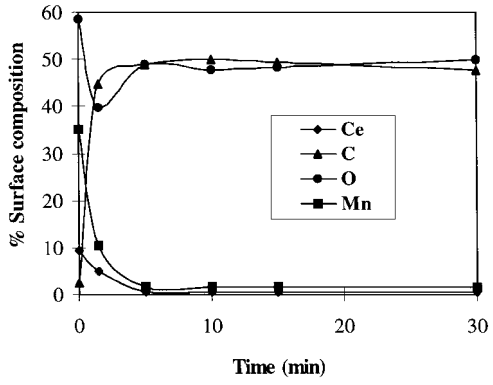

FIG. 11. Relative surface composition of Mn/Ce in the course of WAO reaction. 130°C; 0.5 MPa P_{O_2}.

reactants. The surface content of noble metal, now buried underneath the carbonaceous layer, decreased by a factor of ca. 5. As shown in Table 5, the factor 2 decrease in the aluminum and the oxygen surface concentrations suggests that the major part of the surface carbon species is located on alumina, thus explaining the TPO profile (Fig. 10). In the case of the Mn/Ce catalyst, XPS analyses showed that the carbon content leapt from 2.5% for the fresh catalyst surface to near 50% for the used sample. At the same time, the two metals' relative surface concentrations dramatically dropped from 35 to 1.7% and from 9 to 0.5% for manganese and cerium, respectively.

To follow the formation of the carbonaceous deposit during WAO reaction, a series of XPS analyses were performed on Mn/Ce catalyst samples taken at different reaction times. Typical data are presented in Fig. 11, where the relative surface composition during WAO at 130°C are shown as a function of time on stream. As seen, there is an increase in the carbon content toward a plateau, a slight decrease in the oxygen, and a marked decrease in manganese and cerium contents which reach almost zero after 15 min of WAO reaction. On the other hand, when the ratio of manganese to cerium is plotted against time of reaction at different WAO temperatures (Fig. 12), a common tendency is observed. Mn/Ce ratio decreases, then levels off within 5–10 min of reaction. In addition, the higher the reaction temperature, the higher the ratio, indicating that at lower temperatures, the carbonaceous material is preferentially deposited on cerium oxide sites.

The low decrease in the relative oxygen surface concentration indicates that the carbonaceous material contains oxygenated components. This is consistent with Pintar and Levec (23), who characterized the adsorbed polymer deposits by means of ^{13}C CPMAS NMR and assigned the spectra to a mixture of a copolymer of phenol and glyoxal and a polymer of glyoxal. They estimated from the NMR spectra that the former polymer is predominant. Furthermore, a detailed examination of the C1*s* and O1*s* regions of our XPS spectra reveals a number of overlapping features corresponding to different chemical functionalities. The specific contribution of each functional group can be separated by means of peak reconstruction and curve fitting.

C1s core level. The decomposition of the C1*s* region into individual line components was performed based on reported binding energies for the C1*s* core level for graphitic and oxygen containing carbon species (45, 46). The results obtained and their interpretation are only tentative, and if anything, they demonstrate the complexity of the nature of the deposits. The curve fitting was performed after a Shirley background was subtracted over a constant range of 20 eV. A mixture of Laurentzian and Gaussian curves was used. The FWHM was fixed to 1.5–1.85 eV for the peaks of graphitic and the oxygen-attached carbon, and to 3 eV for the plasmon loss feature (44–47).

Examination of the decomposed C1*s* core level spectra of the platinum/alumina catalyst showed that this region was dominated by a pronounced graphitic peak at B.E. = 284.6 eV (Fig. 13). The carbon species with B.E. < 284 eV were previously assigned to carbidic carbon associated with a form of atomic carbon such as ≡CH or C_{ads} on various surfaces: 283.7 eV on Rh (48); 283.9 eV on Pt (49); 283.2 eV on Pt (46). In this study, the carbidic carbon shoulder occurred at B.E. = 282.9 eV and contributed to only 10.6% of the overall peak, indicating that this constituent is marginal compared to the graphitic peak, which accounts for 54% of the total peak area (Table 6). In fact, Pt is highly favorable to graphite formation, which is in agreement with work on alumina-supported Pt and Ir catalysts by Carter *et al.* (50). The oxygen containing group, mainly from alcohol or ether origin, represented 25% of the total C1*s* peak area.

For the Mn/Ce catalyst, the C1*s* peak reconstruction conducted by using the same criteria as for the platinum catalyst, consisted of four main components, as shown in Table 6. Carbidic peak is precluded, as the catalyst is of an oxide type not able to form carbides. Contrary to the platinum catalyst, the graphitic peak accounted for only

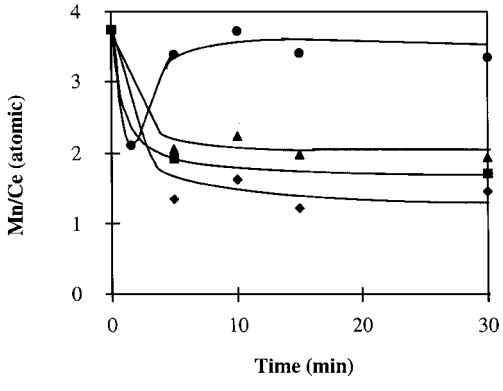

FIG. 12. Mn/Ce surface atomic ratio in the course of WAO at various temperatures: (◆) 80°C; (■) 90°C; (▲) 110°C; (●) 130°C. 0.5 MPa P_{O_2}; catalyst loading = 5 g/L; C_0 = 1 g/L.

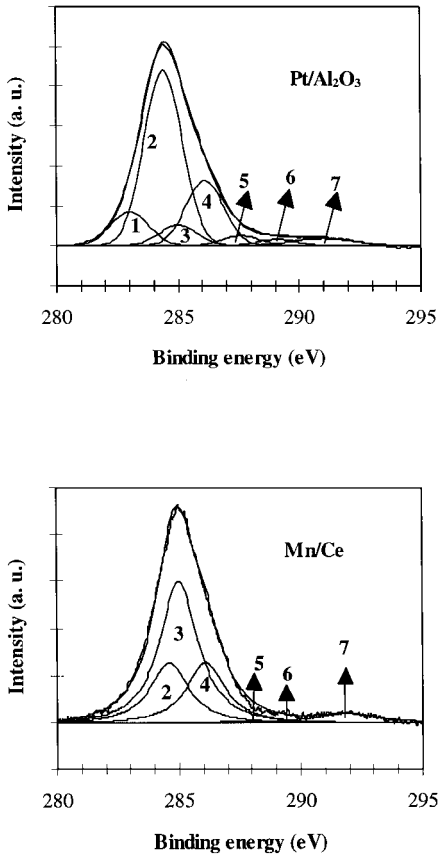

FIG. 13. XP C1*s* spectra of Pt/Al_2O_3 and Mn/Ce after WAO reaction at 130°C, 0.5 MPa P_{O_2}, together with peak line fitting and identification of contributions. (See Table 6 for peak identification.)

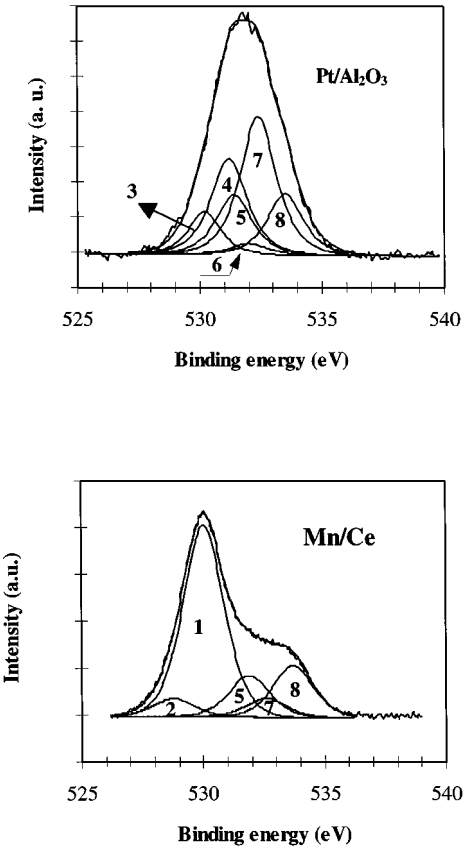

FIG. 14. XP O1*s* spectra of Pt/Al_2O_3 and Mn/Ce after WAO reaction at 130°C, 0.5 MPa P_{O_2}, together with peak line fitting and identification of contributions. (See Table 7 for peak identification.)

one-fifth of the total area, while the highest contribution was recorded for the aliphatic carbon (51%). The contribution of the oxygen containing group was comparable to that of the platinum/alumina catalyst. It is noteworthy to point out the lower level of the graphitic peak which is known to be much more detrimental to the catalyst activity (44). This is also in line with TPO results, which indicated that the carbonaceous material on Mn/Ce catalyst was much more reactive and easier to remove at temperatures below 300°C.

O1s core level. As presented in Fig. 14 and Table 7, the O1*s* spectra were fitted to six specific peaks for the platinum and the Mn/Ce catalysts after reaction at 130°C and 0.5 MPa oxygen pressure. The curve fitting was performed after a Shirley background was subtracted over a constant range

TABLE 6

Binding Energies, Assignments and Peak Areas of C1s Peaks

Peak no.	Binding energy (eV)	Assignment	Area (%) Pt/Al_2O_3	Area (%) Mn/Ce
1	282.9	Carbide	10.6	0
2	284.6	Graphite, aromatics	54.1	21.8
3	285.0	Aliphatics, β-carbons	6.3	51.1
4	286.1	C−OH, C−O−C	20.0	22.0
5	287.6	C=O	3.2	0
6	289.1	COOH, COOR	2.1	0.14
7	291.2	Plasmon loss	3.8	5.1

Note. WAO temperature: 130°C; P_{O_2}: 0.5 MPa; reaction time: 2 h for Pt/Al_2O_3 and 30 min for Mn/Ce.

TABLE 7

Binding Energies, Assignments, and Peak Areas of O1s Peaks

Peak no.	Binding energy (eV)	Assignment	Area (%) Pt/Al_2O_3	Area (%) Mn/Ce
1	528.6	CeO_2	—	5.5
2	529.8	MnO_2	—	59.5
3	530.4	PtO	9.4	—
4	531.2	γ-Al_2O_3	23.9	—
5	531.4	OH	14.7	13.0
6	532.0	C=O (C<u>O</u>OR)	2.7	0
7	532.4	H_2O	34.4	5.8
8	533.5	C−O (C−OH; CO<u>O</u>R)	15.0	16.0

Note. WAO temperature: 130°C; P_{O_2}: 0.5 MPa; reaction time: 2 h for Pt/Al_2O_3 and 30 min for Mn/Ce.

of 16 eV. Here also, we were guided by literature data to adjust the positions and FWHM of individual peaks to achieve reasonable fitting. The FWHM was fixed to 1.7 eV according to Paål *et al.* (46, 51). The peaks at B.E. = 531.4 and 532.4 were assigned to surface OH and strongly adsorbed water, respectively (52). The XPS line at B.E. = 531.2 eV is related to γ-Al_2O_3 (53) used as support for the platinum containing catalyst. The peak at 530.4 eV is assigned to PtO (42, 47). However, in the current study, even if the formation of PtO is proposed based on the O1*s* peak reconstruction, this could not be confirmed by a strong shift (3.0 eV) in the Pt4*f* line (54) from metallic Pt to PtO. In fact, the Pt4*f* region which exhibits the strongest signal could not be analyzed due to interference with Al2*p* photoelectron peak. Furthermore, for the Pt4*d* core level used here for quantitative evaluation of the catalyst surface composition, B.E. shifts from metallic Pt to PtO reported in the literature are 1.1 (55), 1.4 (56), and 2.2 eV (57). In the current study the Pt4$d_{5/2}$ XPS line shifted from 314.1 eV for the fresh catalyst to 315.5 eV for the used one. Therefore, the observed shift (1.4 eV) suggests the formation of surface PtO. The carbon-attached oxygen group comprises mostly species with a carbon–oxygen single bond from either an alcohol or an ether. The C=O peak relative area (2.7%) is insignificant and thus excludes the occurrence of ketone intermediates on the platinum catalyst surface, which is in agreement with the C1*s* XPS results. The O[1] and O[2] peaks were assigned to MnO_2 and CeO_2 oxides, respectively (53, 58). In fact, examination of the Mn2*p* and Ce3*d* spectra of a fresh gold sputtered Mn/Ce sample allowed the determination of the oxidation state of surface manganese and cerium oxides. In reference to Au4$f_{7/2}$ XPS line at 84 eV, binding energies of 641.9 and 882.9 eV were found for Mn2$p_{3/2}$ and Ce3$d_{5/2}$ XPS lines, respectively. These values are comparable to those reported by Wagner *et al.* (59) for MnO_2 and CeO_2, i.e., 642.2 and 881.6 eV for Mn2$p_{3/2}$ and Ce3$d_{5/2}$ core levels, respectively. In addition, Imamura *et al.* (21) concluded from the binding energies for the Mn2$p_{3/2}$ and the Ce3$d_{5/2}$ core levels at 642.0 and 883.2 eV, respectively, that the state of surface manganese and cerium oxides prepared by coprecipitation followed by calcination in air, was MnO_2 and CeO_2, respectively. In the case of the Mn/Ce catalyst, the O1*s* peak fitting exhibited a strong signal from the manganese oxide, accounting for more than one-half of the total area of the whole peak. This is followed, in decreasing importance, by surface OH and water, which amount to ca. 20% of the total peak area. The carbon-attached oxygen was exclusively from C–O origin, as indicated by the C1*s* peak reconstruction results.

CONCLUSION

The catalytic oxidation of phenol in aqueous solutions was investigated in the presence of Pt/Al_2O_3 and Mn/Ce catalysts. The platinum containing catalyst exhibited lower activity in comparison to the Mn/Ce composite oxide catalyst. Phenol conversion over Pt/Al_2O_3 after 1 h reaction was 50% at 130°C and 95% at 175°C. In the presence of Mn/Ce, complete removal of phenol was achieved within 30 min reaction at 130°C, and within 2 h at 80°C, demonstrating the high potential of this catalyst.

The current work showed that during the wet oxidation reaction, some products underwent strong adsorption on the catalyst surface. From the TPO-MS analyses, a net difference was observed in the combustion behavior of the organic deposit depending on the type of catalyst used. From the XPS analyses, the organic overlayer was found to be mainly graphitic for the platinum/alumina catalyst and aliphatic for the Mn/Ce. The presence of oxygen containing organic material on both catalysts surfaces was also demonstrated.

To benefit from the potential advantages of heterogeneously catalyzed WAO process operated under very mild reaction conditions compared to conventional WAO, it is essential to develop catalysts resistant to fouling. Understanding the phenomena occurring at the catalyst surface during WAO reactions may lead to the development of appropriate strategies to eliminate or at least minimize the effect of catalyst deactivation.

ACKNOWLEDGMENTS

Financial support from the Natural Sciences and Engineering Research Council of Canada (NSERC) and the Fonds pour la Formation de Chercheurs et d'Aide à la Recherche (Québec) is gratefully acknowledged. The authors thank Dr. A. Adnot for taking the XPS spectra and providing helpful references, and Professor B. Grandjean for lending us the Leybold mass spectrometer.

REFERENCES

1. Dohnal, V., and Fenclová, D., *J. Chem. Eng. Data* **40**, 478 (1995).
2. Randall, T. L., and Knopp, P. V., *J. Water Pollut. Control Fed.* **52**, 2117 (1980).
3. Heimbuch, J. A., and Wilhelmi, A. R., *J. Hazard. Mater.* **12**, 187 (1985).
4. Gitchel, W. B., Meidl, J. A., and Burant, W., Jr., *AIChE Symp. Ser.* **151**(71), 414 (1975).
5. Charest, F., and Chornet, E., *Can. J. Chem. Eng.* **54**, 190 (1976).
6. Perrich, J. R. (Ed.), "CRC Handbook of Activated Carbon Adsorption for Wastewater Treatment." CRC Press, Boca Raton, FL, 1981.
7. Dietrich, M. J., Randall, T. L., and Canney, P. J., *Env. Prog.* **4**(3), 171 (1985).
8. Pruden, B. B., and Le, H., *Can. J. Chem. Eng.* **54**, 319 (1976).
9. Ito, M. M., Akita, K., and Inoue, H., *Ind. Eng. Chem. Res.* **28**, 894 (1989).
10. Mishra, V. S., Mahajani, V. V., and Joshi, J. B., *Ind. Eng. Chem. Res.* **34**, 2 (1995).
11. Chowdhury, A. K., and Ross, L. W., *AIChE. Symp. Ser.* **151**(71), 46 (1975).
12. Imamura, S., Hirano, A., and Kawabata, N., *Ind. Eng. Chem. Prod. Res. Dev.* **21**, 570 (1982).
13. Kulkarni, U. S., and Dixit, S. G., *Ind. Eng. Chem. Res.* **30**, 1916 (1991).
14. Shende, R. V., and Mahajani, V. V., *Ind. Eng. Chem. Res.* **33**, 3125 (1994).

15. Lin, S. H., Ho, S. J., and Wu, C. L., *Ind. Eng. Chem. Res.* **35**, 307 (1996).
16. Gallezot, P., Chaumet, S., Perrard, A., and Isnard, P., *J. Catal.* **168**, 104 (1997).
17. Sadana, A., and Katzer, J. R., *J. Catal.* **35**, 140 (1974).
18. Sadana, A., and Katzer, J. R., *Ind. Eng. Chem. Fundam.* **13**(2), 127 (1974).
19. Box, E. O., and Farha, F., "Polluted Water Purification," U.S. Patent 3,823,088, 1974.
20. Imamura, S., Dol, A., and Ishida, S., *Ind. Eng. Chem. Prod. Res. Dev.* **24**, 75 (1985).
21. Imamura, S., Nakamura, M., Kawabata, N., Yoshida, J., and Ishida, S., *Ind. Eng. Chem. Prod. Res. Dev.* **25**, 34 (1986).
22. Levec, J., *Appl. Catal.* **63**, L1 (1990).
23. Pintar, A., and Levec, J., *J. Catal.* **135**, 345 (1992).
24. Okitsu, K., Higashi, K., Nagata, Y., Dohmaru, T., Takenaka, N., Bandow, H., and Maeda, Y., *Nippon Kagaku Kaishi* **3**, 208 (1995).
25. Mantzavinos, D., Hellenbrand, R., Livingston, A. G., and Metcalfe, I. S., *Appl. Catal. B* **7**, 379 (1996).
26. Gallezot, P., Laurain, N., and Isnard, P., *Appl. Catal. B* **9**, L11 (1996).
27. Doraiswamy, L. K., and Sharma, M. M., "Heterogeneous Reactions: Analysis, Examples and Reactor Design. Volume 2: Fluid-Fluid-Solid Reactions," p. 283. Wiley, New York, 1984.
28. Matatov-Meytal, Y. I., and Sheintuch, S., *Ind. Eng. Chem. Res.* **37**, 309 (1998).
29. Smith, J. M., "Chemical Engineering Kinetics," 3rd ed., p. 486. McGraw–Hill, New York, 1981.
30. Thomas, J. M., and Thomas, W. J., "Principles and Practice of Heterogeneous Catalysis." VCH Verlag, Weinheim, 1997.
31. Devlin, H. R., and Harris, I. J., *Ind. Eng. Chem. Fundam.* **23**, 387 (1984).
32. Joglekar, M. S., Samant, S. D., and Joshi, J. B., *Wat. Res.* **25**, 135 (1991).
33. Atwater, J. E., Akse, J. R., McKinnis, J. A., and Thompson, O. T., *Appl. Catal. B* **11**, L11 (1996).
34. Donlagic, J., and Levec, J., *Ind. Eng. Chem. Res.* **36**(9), 3480 (1997).
35. Mantzavinos, D., Hellenbrand, R., Livingston, A. G., and Metcalfe, I. S., *Trans. I. Chem. E.* **75**, 87 (1997).
36. Pintar, A., and Levec, J., *Chem. Eng. Sci.* **47**(9–11), 2395 (1992).
37. Menon, P. G., *Chem. Rev.* **94**, 1021 (1994).
38. Christensen, T. S., and Rosturp-Nielsen, J., "Deactivation and Testing of Hydrocarbon-Processing Catalysts" (P. O'Connor, T. Takatsuka, and G. L. Woolery, Eds.), p. 186, ACS Symp. Ser. No. 634. Am. Chem. Soc., Washington, DC, 1996.
39. Bond, G. C., Dias, C., and Portela, M. F., *J. Catal.* **156**, 295 (1995).
40. Parera, J. M., Figoli, N. S., and Traffano, E. M., *J. Catal.* **79**, 481 (1983).
41. Barbier, J., Corro, G., and Zhang, Y., *Appl. Catal.* **16**, 169 (1985).
42. Augustine, S. M., Alameddin, G. N., and Sachtler, W. M. H., *J. Catal.* **115**, 217 (1989).
43. Pieck, C. L., Verderone, R. J., Jablonski, E. L., and Parera, J. M., *Appl. Catal.* **55**, 1 (1989).
44. Menon, P. G., *J. Mol. Catal.* **59**, 207 (1990).
45. Desimoni, E., Casella, G. I., Morone, A., and Salvi, A. M., *Surf. Interface. Anal.* **15**, 627 (1990).
46. Paál, Z., Schlögl, R., and Ertl, G., *Catal. Lett.* **12**, 331 (1992).
47. Darmstadt, H., Roy, C., and Kaliaguine, S., *Carbon* **32**(8), 1399 (1994).
48. Levis, R. J., DeLouise, L. A., White, E. J., and Winograd, N., *Surf. Sci.* **230**, 35 (1990).
49. Belton, D. N., and Schmieg, S. J., *Surf. Sci.* **233**, 131 (1990).
50. Carter, J. L., McVicker, G. B., Weissman, W., Kmak, W. S., and Sinfelt, J. H., *Appl. Catal.* **3**, 327 (1982).
51. Paál, Z., Schlögl, R., and Ertl, G., *J. Chem. Soc. Faraday. Trans. I* **88**(8), 1179 (1992).
52. Kiskinova, M., Pirug, G., and Bonzel, H. P., *Surf. Sci.* **160**, 319 (1985).
53. Wagner, C. D., Zatko, D. A., and Raymond, R. H., *Anal. Chem.* **52**(9), 1445 (1980).
54. Wagner, C. D., "Practical Surface Analysis" (D. Briggs and M. P. Seah, Eds.), 2nd ed., Vol. 1, p. 621. Wiley, Chichester, UK, 1990.
55. Shyu, J. Z., and Otto, K., *Appl. Surf. Sci.* **32**, 546 (1988).
56. Vedrine, J. C., Dufaux, M., Naccache, C., and Imelik, B., *J. Chem. Soc. Faraday. Trans. I* **74**, 440 (1978).
57. Rossin, J. A., *J. Mol. Catal.* **58**, 363 (1990).
58. Bensalem, A., Bozon-Verduraz, F., Delamar, M., and Bugli, G., *Appl. Catal. A* **121**, 81 (1995).
59. Wagner, C. D., Riggs, W. M., Davis, L. E., Moulder, J. F., and Muilenberg, G. E., "Handbook of X-Ray Photoelectron Spectroscopy." Perkin–Elmer Corporation, Physical Electronics Division, Eden Prairie, MS, 1979.